NASA / CR-1998-206950

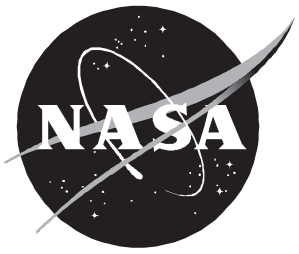

Application of Model Based Parameter Estimation for Fast Frequency Response Calculations of Input Characteristics of Cavity-Backed Aperture Antennas Using Hybrid FEM / MoM Technique

C. J. Reddy
Hampton University, Hampton, Virginia

March 1998

The NASA STI Program Office . . . in Profile

Since its founding, NASA has been dedicated to the advancement of aeronautics and space science. The NASA Scientific and Technical Information (STI) Program Office plays a key part in helping NASA maintain this important role.

The NASA STI Program Office is operated by Langley Research Center, the lead center for NASA's scientific and technical information. The NASA STI Program Office provides access to the NASA STI Database, the largest collection of aeronautical and space science STI in the world. The Program Office is also NASA's institutional mechanism for disseminating the results of its research and development activities. These results are published by NASA in the NASA STI Report Series, which includes the following report types:

- TECHNICAL PUBLICATION. Reports of completed research or a major significant phase of research that present the results of NASA programs and include extensive data or theoretical analysis. Includes compilations of significant scientific and technical data and information deemed to be of continuing reference value. NASA counter-part or peer-reviewed formal professional papers, but having less stringent limitations on manuscript length and extent of graphic presentations.

- TECHNICAL MEMORANDUM. Scientific and technical findings that are preliminary or of specialized interest, e.g., quick release reports, working papers, and bibliographies that contain minimal annotation. Does not contain extensive analysis.

- CONTRACTOR REPORT. Scientific and technical findings by NASA-sponsored contractors and grantees.

- CONFERENCE PUBLICATION. Collected papers from scientific and technical conferences, symposia, seminars, or other meetings sponsored or co-sponsored by NASA.

- SPECIAL PUBLICATION. Scientific, technical, or historical information from NASA programs, projects, and missions, often concerned with subjects having substantial public interest.

- TECHNICAL TRANSLATION. English-language translations of foreign scientific and technical material pertinent to NASA's mission.

Specialized services that help round out the STI Program Office's diverse offerings include creating custom thesauri, building customized databases, organizing and publishing research results . . . even providing videos.

For more information about the NASA STI Program Office, see the following:

- Access the NASA STI Program Home Page at ***http://www.sti.nasa.gov***

- Email your question via the Internet to help@sti.nasa.gov

- Fax your question to the NASA Access Help Desk at (301) 621-0134

- Phone the NASA Access Help Desk at (301) 621-0390

- Write to:
  NASA Access Help Desk
  NASA Center for AeroSpace Information
  800 Elkridge Landing Road
  Linthicum Heights, MD 21090-2934

NASA / CR-1998-206950

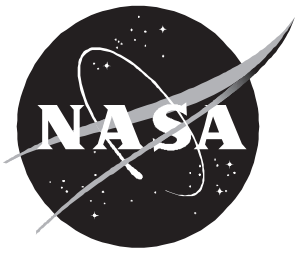

Application of Model Based Parameter Estimation for Fast Frequency Response Calculations of Input Characteristics of Cavity-Backed Aperture Antennas Using Hybrid FEM / MoM Technique

C. J. Reddy
Hampton University, Hampton, Virginia

National Aeronautics and
Space Administration

Langley Research Center
Hampton, Virginia 23681-2199

Prepared for Langley Research Center
under Cooperative Agreement NCC1-231

March 1998

Available from the following:

NASA Center for AeroSpace Information (CASI)
800 Elkridge Landing Road
Linthicum Heights, MD 21090-2934
(301) 621-0390

National Technical Information Service (NTIS)
5285 Port Royal Road
Springfield, VA 22161-2171
(703) 487-4650

CONTENTS

Abstract

Model Based Parameter Estimation (MBPE) is presented in conjunction with the hybrid Finite Element Method (FEM)/Method of Moments (MoM) technique for fast computation of the input characteristics of cavity-backed aperture antennas over a frequency range. The hybrid FEM/ MoM technique is used to form an integro-partial-differential equation to compute the electric field distribution of a cavity-backed aperture antenna. In MBPE, the electric field is expanded in a rational function of two polynomials. The coefficients of the rational function are obtained using the frequency derivatives of the integro-partial-differential equation formed by the hybrid FEM/ MoM technique. Using the rational function approximation, the electric field is obtained over a frequency range. Using the electric field at different frequencies, the input characteristics of the antenna are obtained over a wide frequency range. Numerical results for an open coaxial line, probe-fed coaxial cavity and cavity-backed microstrip patch antennas are presented. Good agreement between MBPE and the solutions over individual frequencies is observed.

List of Symbols

∇	Del operator
∇'	Del operator over the source coordinates
ε_r	Dielectric permittivity of the medium in the cavity
ε_{rc}	Dielectric permittivity of the medium in the coaxial feed line
δ_{qo}	Kronecker delta defined in equation (22)
μ_r	Dielectric permeability of the medium in the cavity
ρ	ρ-coordinate of the cylindrical coordinate system
$\hat{\rho}$	Unit normal vector along the ρ-axis
ω	Angular frequency
AWE	Asymptotic Waveform Evaluation
MBPE	Model Based Parameter Estimation
$A^{(q)}(k_o)$	q^{th} derivative of $A(k)$ with respect to k; $\frac{d^q}{dk^q}A(k)$, evaluated at k_o
a_n	Coefficients of the numerator of the rational function $(n = 0, 1, 2, 3, ..., L)$
$B(k)$	Excitation vector
$B^{(q)}(k_o)$	q^{th} derivative of $B(k)$ with respect to k; $\frac{d^q}{dk^q}B(k)$, evaluated at k_o
b_m	Coefficients of the numerator of the rational function $(m = 0, 1, 2, 3, ..., M)$
$C_{r,s}$	Binomial coefficient
ds	Surface integration with respect to observation coordinates
ds'	Surface integration with respect to source coordinates
$\mathbf{E}$	Electric field
$\mathbf{E}_{inp}$	Electric field at the input plane S_{inp}
$e(k)$	Electric field coefficient vector

$\mathbf{e}_{inc}$	Incident electric field due to coaxial line at the surface S_{inp}
$\mathbf{e}_{ref}$	Reflected electric field into the coaxial line at the surface S_{inp}
$\mathbf{H}_{ap}$	Magnetic field at the surface S_{ap}
$\mathbf{H}_{inp}$	Magnetic field at the surface S_{inp}
f	Frequency
j	$\sqrt{-1}$
k	Wavenumber at any frequency f
k_o	Wavenumber at frequency f_o
$\mathbf{M}$	Magnetic current at the surface S_{ap}
$\hat{\mathbf{n}}$	Normal unit vector
$P_L(k)$	Polynomial of order L
$Q_M(k)$	Polynomial of order M
$q!$	Factorial of number q
R_o	Reflection coefficient at the input plane S_{inp}
R	Distance between the source point and the observation point
r_1	Radius of inner conductor of the coaxial feed line
r_2	Radius of outer conductor of the coaxial feed line
$\mathbf{T}$	Vector testing function
$\mathbf{T}_s$	Vector testing function at the surface S_{ap}
Y_{in}	Normalized input admittance of the antenna
$\mathbf{z}$	Unit normal along Z-axis

1. Introduction

Cavity-backed aperture antennas are very popular in aerospace applications due to their conformal nature. Hybrid techniques have become attractive for numerical analysis of these type of problems due to their ability to handle arbitrary shape of the cavity and complex materials that may be required for the antenna design. The combined Finite Element Method (FEM) and Method of Moments (MoM) technique in particular has been used to analyze various cavity-backed aperture antennas[1,2]. In the combined FEM/MoM technique, FEM is used in the cavity volume to compute the electric field, whereas MoM is used to compute the magnetic current at the aperture. Using Galerkin's technique, an integro-partial-differential equation is formed. The cavity is divided into tetrahedral elements and the aperture is discretized by triangles. Simultaneous equations are generated over the subdomains and are added to form a global matrix equation. This results in a partly sparse and partly dense symmetric complex matrix, which can be solved either by a direct solver or by an iterative solver. The electric field hence obtained is used to compute the radiation characteristics and input characteristics of the antenna.

In most practical applications, input characteristics such as input impedance or input admittance are of interest over a frequency range. To obtain the frequency response of the antenna, one has to repeat the above calculations at every incremental frequency over the frequency band of interest. If the antenna is highly frequency dependent, one needs to do the calculations at fine increments of frequency to get an accurate representation of the frequency response. For electrically large cavities with large apertures, this can be computationally intensive and in some cases computationally prohibitive. To alleviate the above problems, recently Asymptotic Waveform Evaluation (AWE) was applied to frequency domain electromagnetics to obtain the frequency response[3-6]. In AWE, the unknown electric field was expanded in Taylor

series around a frequency. The coefficients of Taylor series were obtained using the frequency derivatives of the integro-partial-differential equation resulting from the combined FEM/MoM technique[6].

In this report, a similar but more flexible method called *Model Based Parameter Estimation* (MBPE)[7,8] is applied for predicting the input characteristics of cavity-backed aperture antennas over a wide band of frequencies using the combined FEM/MoM technique. In MBPE technique, the electric field is expanded as a rational function. The coefficients of the rational function are obtained using the frequency data and the frequency derivative data. Once the coefficients of the rational function are obtained, the electric field in the cavity can be obtained at any frequency within the frequency range. Using the electric field, the input characteristics such as the input impedance or admittance can be calculated. If the frequency derivative information is known for more than one frequency, a rational function matching all the samples can be obtained resulting in a wider frequency response.

The rest of the report is organized as follows. In section 2, MBPE implementation for the combined FEM/MoM technique is described. Numerical results for an open coaxial line, a coaxial cavity fed by a coaxial line and cavity-backed microstrip patch antennas are presented in section 3. The numerical data are compared with the exact solution over the bandwidth. CPU timings are given for each example. Concluding remarks on the advantages and disadvantages of MBPE are given in section 4.

2. MBPE Implementation for the combined FEM/MoM Technique

The geometry of the problem to be analyzed is shown in Figure 1. For linear, isotropic, and source free region, the electric field satisfies the vector wave equation:

$$\nabla\times\left(\frac{1}{\mu_r}\nabla\times\mathbf{E}\right)-k^2\varepsilon_r\mathbf{E}\;=\;0 \tag{1}$$

where μ_r, ε_r are the relative permeability and relative permittivity of the medium in the cavity. The time variation $\exp(j\omega t)$ is assumed and suppressed throughout this report. Applying the Galerkin's technique, equation (1) can be written in "weak form" as [1]

$$\iiint_V (\nabla\times\mathbf{T})\bullet\left(\frac{1}{\mu_r}\nabla\times\mathbf{E}\right)dv-k^2\varepsilon_r\iiint_V\mathbf{T}\bullet\mathbf{E}\,dv-j\omega\mu_o\iint_{S_{ap}}(\mathbf{T}\times\hat{\mathbf{n}})\bullet\mathbf{H}_{ap}ds$$

$$=\quad j\omega\mu_o\iint_{S_{inp}}\mathbf{T}\bullet(\hat{\mathbf{n}}\times\mathbf{H}_{inp})ds \tag{2}$$

where $\mathbf{T}$ is the vector testing function, S_{ap} is the aperture surface, and S_{inp} is the input surface (see fig. 1). $\mathbf{H}_{ap}$ is the magnetic field at the aperture and $\mathbf{H}_{inp}$ is the magnetic field at the input surface.

In accordance with the equivalence principle [9], the fields inside the cavity can be decoupled to the fields outside the cavity by closing the aperture with a Perfect Electric Conductor (PEC) and introducing the equivalent magnetic current.

$$\mathbf{M}\;=\;\mathbf{E}\times\hat{\mathbf{z}} \tag{3}$$

over the extent of the aperture. Making use of the image theory, the integrals over S_{ap} in equation (2) can be written as

$$j\omega\mu_o \int\int_{S_{ap}} (\mathbf{T}\times\hat{\mathbf{n}})\bullet\mathbf{H}_{ap}\,ds$$

$$= \frac{k^2}{2\pi}\int\int_{S_{ap}} \mathbf{T}_s \bullet \left(\int\int_{S_{ap}} \mathbf{M}\frac{\exp(-jkR)}{R}ds'\right)ds$$

$$-\frac{1}{2\pi}\int\int_{S_{ap}} (\nabla\bullet\mathbf{T}_s)\left\{\int\int_{S_{ap}} (\nabla'\bullet\mathbf{M})\frac{\exp(-jkR)}{R}ds'\right\}ds \qquad (4)$$

where $\mathbf{T}_s = \mathbf{T}\times\hat{\mathbf{n}}$ and R is the distance between source point and the observation point. ∇' indicates del operation over the source coordinates and ds' indicates the surface integration over the source region.

Though the analysis presented in this report is not limited to any specific input feed structure, we restrict the presentation of the formulation to the coaxial line as the input feed structure. The cross section of the coaxial line is shown in Figure 2. Assuming that the incident electric field is the transverse electromagnetic (TEM) mode and the reflected field also consists of TEM mode only, the electric field at the input plane S_{inp} is given by

$$\mathbf{E}_{inp} = \mathbf{e}_{inc}\exp(-jk\sqrt{\varepsilon_{rc}}z) + \mathbf{e}_{ref}\exp(jk\sqrt{\varepsilon_{rc}}z) \qquad (5)$$

where

$$\mathbf{e}_{inc} = \hat{\rho}\frac{1}{\sqrt{2\pi\ln\left(\frac{r_2}{r_1}\right)}}\frac{1}{\rho} \qquad (6)$$

and

$$\mathbf{e}_{ref} = R_o\mathbf{e}_{inc} \qquad (7)$$

R_o is the reflection coefficient and is given by

$$R_o = \frac{\exp(-jk\sqrt{\varepsilon_{rc}}z_1)}{\sqrt{2\pi\ln\left(\frac{r_2}{r_1}\right)}}\int\int_{S_{inp}} \mathbf{E}\bullet\left(\frac{\hat{\rho}}{\rho}\right)ds - \exp(-2jk\sqrt{\varepsilon_{rc}}z_1) \qquad (8)$$

r_2 is the outer radius and r_1 is the inner radius of the coaxial line. ε_{rc} is the relative permittivity of the coaxial line.

Using equation (5) to calculate $\mathbf{H}_{inp}$, the surface integral over S_{inp} in equation (2) can be written as

$$j\omega\mu_o \int\int_{S_{inp}} \mathbf{T} \bullet (\hat{\mathbf{n}} \times \mathbf{H}_{inp}) ds$$

$$= \frac{-jk\sqrt{\varepsilon_{rc}}}{2\pi \ln\left(\frac{r_2}{r_1}\right)\mu_{rc}} \left\{ \int\int_{S_{inp}} \mathbf{T} \bullet \left(\frac{\hat{\rho}}{\rho}\right) ds \right\} \left\{ \int\int_{S_{inp}} \mathbf{E} \bullet \left(\frac{\hat{\rho}}{\rho}\right) ds \right\}$$

$$+ \frac{2jk\sqrt{\varepsilon_{rc}} \exp(-jk\sqrt{\varepsilon_{rc}} z_1)}{\mu_{rc}\sqrt{2\pi \ln\left(\frac{r_2}{r_1}\right)}} \int\int_{S_{inp}} \mathbf{T} \bullet \left(\frac{\hat{\rho}}{\rho}\right) ds \qquad (9)$$

Substituting equation (4) and (8) in equation (2), the system equations for the combined FEM/ MoM technique can be written as

$$\iiint_V \frac{1}{\mu_r} (\nabla \times \mathbf{T}) \bullet (\nabla \times \mathbf{E}) dv - k^2 \varepsilon_r \iiint_V \mathbf{T} \bullet \mathbf{E} dv$$

$$- \frac{k^2}{2\pi} \int\int_{S_{ap}} \mathbf{T}_s \bullet \left(\int\int_{S_{ap}} \mathbf{M} \frac{\exp(-jkR)}{R} ds' \right) ds + \frac{1}{2\pi} \int\int_{S_{ap}} (\nabla \bullet \mathbf{T}_s) \left\{ \int\int_{S_{ap}} (\nabla' \bullet \mathbf{M}) \frac{\exp(-jkR)}{R} ds' \right\} ds$$

$$+ \frac{jk\sqrt{\varepsilon_{rc}}}{2\pi \ln\left(\frac{r_2}{r_1}\right)\mu_{rc}} \left\{ \int\int_{S_{inp}} \mathbf{T} \bullet \left(\frac{\hat{\rho}}{\rho}\right) ds \right\} \left\{ \int\int_{S_{inp}} \mathbf{E} \bullet \left(\frac{\hat{\rho}}{\rho}\right) ds \right\}$$

$$= \frac{2jk\sqrt{\varepsilon_{rc}} \exp(-jk\sqrt{\varepsilon_{rc}} z_1)}{\mu_{rc}\sqrt{2\pi \ln\left(\frac{r_2}{r_1}\right)}} \int\int_{S_{inp}} \mathbf{T} \bullet \left(\frac{\hat{\rho}}{\rho}\right) ds \qquad (10)$$

The volume of the cavity is subdivided into small volume tetrahedral elements. The electric field is expressed in terms of the edge vector basis functions [10], which enforce the divergenceless condition of the electric field explicitly. The vector testing function is also expressed in terms of the edge vector basis functions following the Galerkin's method. The discretization of the cavity volume into tetrahedral elements automatically results in discretization of the surfaces S_{ap} and S_{inp} into triangular elements. The volume and surface integrals in equation (10) are carried out over each element to form element matrices and the element matrices are assembled to form global matrices. Equation (10) can be written in matrix form as

$$A(k)e(k) = B(k) \tag{11}$$

$A(k)$ is a partly sparse, partly dense complex symmetric matrix, *B(k)* is the excitation vector, and *e(k)* is the unknown electric field coefficient vector. *A(k)* is evaluated as a sum of three matrices.

$$A(k) = A_1(k) + A_2(k) + A_3(k) + A_4(k) \tag{12}$$

where

$$A_1(k) = \iiint_V \frac{1}{\mu_r}(\nabla\times\mathbf{T})\bullet(\nabla\times\mathbf{E})dv - k^2\varepsilon_r\iiint_V \mathbf{T}\bullet\mathbf{E}dv \tag{13}$$

$$A_2(k) = -\frac{k^2}{2\pi}\iint_{S_{ap}}\mathbf{T}_s\bullet\left(\iint_{S_{ap}}\mathbf{M}\frac{\exp(-jkR)}{R}ds'\right)ds \tag{14}$$

$$A_3(k) = \frac{1}{2\pi}\iint_{S_{ap}}(\nabla\bullet\mathbf{T}_s)\left\{\iint_{S_{ap}}(\nabla'\bullet\mathbf{M})\frac{\exp(-jkR)}{R}ds'\right\}ds \tag{15}$$

$$A_4(k) = \frac{jk\sqrt{\varepsilon_{rc}}}{2\pi\ln\left(\frac{r_2}{r_1}\right)\mu_{rc}}\left\{\iint_{S_{inp}}\mathbf{T}\bullet\left(\frac{\hat{\rho}}{\rho}\right)ds\right\}\left\{\iint_{S_{inp}}\mathbf{E}\bullet\left(\frac{\hat{\rho}}{\rho}\right)ds\right\} \tag{16}$$

$$B(k) = \frac{2jk\sqrt{\varepsilon_{rc}}\exp(-jk\sqrt{\varepsilon_{rc}}z_1)}{\mu_{rc}\sqrt{2\pi\ln\left(\frac{r_2}{r_1}\right)}}\int\int_{S_{inp}} \mathbf{T}\bullet\left(\frac{\hat{\rho}}{\rho}\right)ds \tag{17}$$

The matrix equation (11) is solved at any specific frequency, f_o (with wavenumber k_o) either by a direct method or by an iterative method. The solution of the equation (11) gives the unknown electric field coefficients which are used to obtain the electric field distribution. Once the electric field distribution is known, the input reflection coefficient can be calculated using equation (8). The input plane is placed at $z_1 = 0$, and the reflection coefficient is calculated as

$$\Gamma = R_o\big|_{z_1=0} = \frac{1}{\sqrt{2\pi\ln\left(\frac{r_2}{r_1}\right)}}\int\int_{S_{inp}} \mathbf{E}\bullet\left(\frac{\hat{\rho}}{\rho}\right)ds - 1 \tag{18}$$

The normalized input admittance at S_{inp} is given by

$$Y_{in} = \frac{1-\Gamma}{1+\Gamma} \tag{19}$$

The input admittance given in equation (18) is calculated at one frequency. If one needs the input admittance over a frequency range, this calculation is to be repeated at different frequency values. Instead MBPE [7,8] can be applied for rapid calculation of input admittance/ impedance over a frequency range. MBPE technique involves expanding the unknown coefficient vector as a rational polynomial. The coefficients of the rational polynomial are obtained by matching the function and its frequency derivatives of the function at one or more frequency points.

The solution of equation (11) at any frequency f_o gives the unknown electric field coefficient column vector $e(k_o)$, where k_o is the free space wavenumber at f_o. Instead $e(k)$ can be written as a rational function,

$$e(k) = \frac{P_L(k)}{Q_M(k)} \tag{20}$$

where

$$P_L(k) = a_o + a_1 k + a_2 k^2 + a_3 k^3 + \ldots\ldots\ldots\ldots + a_L k^L$$

$$Q_M(k) = b_o + b_1 k + b_2 k^2 + b_3 k^3 + \ldots\ldots\ldots\ldots + b_M k^M$$

b_o is set to 1 as the rational function can be divided by an arbitrary constant. The coefficients of the rational function are obtained by matching the frequency-derivatives of *e(k).* If equation (14) is differentiated *t* times with respect to *k*, the resulting equations can be written as [8]

$$eQ_M = P_L$$

$$e'Q_M + eQ_M' = P_L'$$

$$e''Q_M + 2e'Q_M' + eQ_M'' = P_L''$$

$$e'''Q_M + 3e''Q_M' + 3e'Q_M'' + eQ_M''' = P_L'''$$

.
.
.

$$e^{(t)}Q_M + te^{(t-1)}Q_M^{(1)} + \ldots\ldots\ldots\ldots + C_{t,\,t-m}e^{(m)}Q^{(t-m)} + \ldots\ldots\ldots\ldots + eQ_M^{(t)} = P_L^{(t)}$$

where $C_{r,s} = \frac{r!}{s!(r-s)!}$ is the binomial coefficient. The system of *(t+1)* equations provides the information from which the rational function coefficients can be found if $t \geq L + M + 1$. If the frequency derivatives are available at only one frequency f_o, the variable in the rational function can be replaced with $(k - k_o)$ i.e.,

$$e(k) = \frac{P_L(k - k_o)}{Q_M(k - k_o)} \tag{21}$$

and the derivatives can be evaluated at $k = k_o$. The coefficients of the rational function can be obtained from the following equations:

$$a_o = e(k_o) \tag{22}$$

$$\begin{bmatrix} 1 & ..... & -e_o & 0 & ..... & 0 \\ 0 & ..... & -e_1 & -e_o & ..... & 0 \\ 0 & ..... & -e_2 & -e_1 & & 0 \\ 0 & ..... & -e_3 & -e_2 & & 0 \\ \cdots & \cdots & \cdots & \cdots & \cdots & \cdots \\ 0 & ..... & -e_{L+M-1} & e_{L+M-2} & .... & -e_L \end{bmatrix} \begin{bmatrix} a_1 \\ a_2 \\ \cdots \\ a_L \\ \cdots \\ b_M \end{bmatrix} = \begin{bmatrix} e_1 \\ e_2 \\ \cdots \\ e_L \\ \cdots \\ e_{L+M} \end{bmatrix} \tag{23}$$

where $e_m = \dfrac{e^{(m)}}{m!}$. For example for a rational function with *L=5* and *M=4*, the matrix equation can be written as

$$\begin{bmatrix} 1 & 0 & 0 & 0 & 0 & -e_o & 0 & 0 & 0 \\ 0 & 1 & 0 & 0 & 0 & -e_1 & -e_0 & 0 & 0 \\ 0 & 0 & 1 & 0 & 0 & -e_2 & -e_1 & -e_0 & 0 \\ 0 & 0 & 0 & 1 & 0 & -e_3 & -e_2 & -e_1 & -e_0 \\ 0 & 0 & 0 & 0 & 1 & -e_4 & -e_3 & -e_2 & -e_1 \\ 0 & 0 & 0 & 0 & 0 & -e_5 & -e_4 & -e_3 & -e_2 \\ 0 & 0 & 0 & 0 & 0 & -e_6 & -e_5 & -e_4 & e_3 \\ 0 & 0 & 0 & 0 & 0 & -e_7 & -e_6 & -e_5 & -e_4 \\ 0 & 0 & 0 & 0 & 0 & -e_8 & -e_7 & -e_6 & -e_5 \end{bmatrix} \begin{bmatrix} a_1 \\ a_2 \\ a_3 \\ a_4 \\ a_5 \\ b_1 \\ b_2 \\ b_3 \\ b_4 \end{bmatrix} = \begin{bmatrix} e_1 \\ e_2 \\ e_3 \\ e_4 \\ e_5 \\ e_6 \\ e_7 \\ e_8 \\ e_9 \end{bmatrix} \tag{24}$$

This approach is same as the Padé approximation given in [3]. This method has been successfully applied to electromagnetic scattering from cavity-backed apertures using a hybrid finite element and method of moments technique[11].

If the frequency derivatives are known at more than one frequency, then the expansion about $k=k_o$ cannot be used and the system matrix to solve the rational function coefficients takes a general form [8]. For the sake of simplicity, only a two frequency model is presented here. Assume that at two frequencies, f_1 (with free space wavenumber k_1) and f_2 (with free space wavenumber k_2), four derivatives are evaluated at each frequency. Hence 10 samples of data are available (two frequency samples and a total of eight frequency derivative samples) to form a rational function with $L=5$ and $M=4$

$$e(k) = \frac{a_o + a_1 k + a_2 k^2 + a_3 k^3 + a_4 k^4 + a_5 k^5}{1 + b_1 k + b_2 k^2 + b_3 k^3 + b_4 k^4} \tag{25}$$

Equation (25) can be written as

$$(1 + b_1 k + b_2 k^2 + b_3 k^3 + b_4 k^4) e(k) = a_o + a_1 k + a_2 k^2 + a_3 k^3 + a_4 k^4 + a_5 k^5 \tag{26}$$

Differentiating equation (26) four times at each frequency, the matrix equation for the solution of the coefficients of the rational function (equation (25)) can be written as

$$\begin{bmatrix}
1 & k_1 & k_1^2 & k_1^3 & k_1^4 & k_1^5 & e_1^{(0)}k_1 & e_1^{(0)}k_1^2 & e_1^{(0)}k_1^3 & e_1^{(0)}k_1^4 \\
0 & 1 & 2k_1 & 3k_1^2 & 4k_1^3 & 5k_1^4 & M_{27} & M_{28} & M_{29} & M_{2\ 10} \\
0 & 0 & 2 & 6k_1 & 12k_1^2 & 20k_1^3 & M_{37} & M_{38} & M_{39} & M_{3\ 10} \\
0 & 0 & 0 & 6 & 24k_1 & 60k_1^2 & M_{47} & M_{48} & M_{49} & M_{4\ 10} \\
0 & 0 & 0 & 0 & 24 & 120k_1 & M_{57} & M_{58} & M_{59} & M_{5\ 10} \\
1 & k_2 & k_2^2 & k_2^3 & k_2^4 & k_2^5 & e_2^{(0)}k_2 & e_2^{(0)}k_2^2 & e_2^{(0)}k_2^3 & e_2^{(0)}k_2^4 \\
0 & 1 & 2k_2 & 3k_2^2 & 4k_2^3 & 5k_2^4 & M_{77} & M_{78} & M_{79} & M_{7\ 10} \\
0 & 0 & 2 & 6k_2 & 12k_2^2 & 20k_2^3 & M_{87} & M_{88} & M_{89} & M_{8\ 10} \\
0 & 0 & 0 & 6 & 24k_2 & 60k_2^2 & M_{97} & M_{98} & M_{99} & M_{9\ 10} \\
0 & 0 & 0 & 0 & 24 & 120k_2 & M_{10\ 7} & M_{10\ 8} & M_{10\ 9} & M_{10\ 10}
\end{bmatrix}
\begin{bmatrix} a_o \\ a_1 \\ a_2 \\ a_3 \\ a_4 \\ a_5 \\ b_1 \\ b_2 \\ b_3 \\ b_4 \end{bmatrix}
=
\begin{bmatrix} e_1^{(0)} \\ e_1^{(1)} \\ e_1^{(2)} \\ e_1^{(3)} \\ e_1^{(4)} \\ e_2^{(0)} \\ e_2^{(1)} \\ e_2^{(2)} \\ e_2^{(3)} \\ e_2^{(4)} \end{bmatrix} \tag{27}$$

where $e_1^{(m)} = \frac{d^m}{dk^m} e(k)\big|_{k=k_1}$, $e_2^{(m)} = \frac{d^m}{dk^m} e(k)\big|_{k=k_2}$ and

$$M_{27} = -(e_1^{(1)} k_1 + e_1^{(0)})$$

$$M_{28} = -(e_1^{(1)} k_1^2 + 2e_1^{(0)} k_1)$$

$$M_{29} = -(e_1^{(1)} k_1^3 + 3e_1^{(0)} k_1^2)$$

$$M_{2\ 10} = -(e_1^{(1)} k_1^4 + 4e_1^{(0)} k_1^3)$$

$$M_{37} = -(e_1^{(2)} k_1 + 2e_1^{(1)})$$

$$M_{38} = -(e_1^{(2)} k_1^2 + 4e_1^{(1)} k_1 + 2e_1^{(0)})$$

$$M_{39} = -(e_1^{(2)} k_1^3 + 6e_1^{(1)} k_1^2 + 6e_1^{(0)} k_1)$$

$$M_{3\ 10} = -(e_1^{(2)} k_1^4 + 8e_1^{(1)} k_1^3 + 12e_1^{(0)} k_1^2)$$

$$M_{47} = -(e_1^{(3)} k_1 + 3e_1^{(2)})$$

$$M_{48} = -(e_1^{(3)} k_1^2 + 6e_1^{(2)} k_1 + 6e_1^{(1)})$$

$$M_{49} = -(e_1^{(3)} k_1^3 + 9e_1^{(2)} k_1^2 + 18e_1^{(1)} k_1 + 6e_1^{(0)})$$

$$M_{4\ 10} = -(e_1^{(3)} k_1^4 + 12e_1^{(2)} k_1^3 + 36e_1^{(1)} k_1^2 + 24e_1^{(0)} k_1)$$

$$M_{57} = -(e_1^{(4)} k_1 + 4e_1^{(3)})$$

$$M_{58} = -(e_1^{(4)} k_1^2 + 8e_1^{(3)} k_1 + 12e_1^{(2)})$$

$$M_{59} = -(e_1^{(4)}k_1^3 + 12e_1^{(3)}k_1^2 + 36e_1^{(2)}k_1 + 24e_1^{(0)})$$

$$M_{5\ 10} = -(e_1^{(4)}k_1^4 + 16e_1^{(3)}k_1^3 + 72e_1^{(2)}k_1^2 + 96e_1^{(1)}k_1 + 24e_1^{(0)})$$

$$M_{77} = -(e_2^{(1)}k_2 + e_2^{(0)})$$

$$M_{78} = -(e_2^{(1)}k_2^2 + 2e_2^{(0)}k_2)$$

$$M_{78} = -(e_2^{(1)}k_2^3 + 3e_2^{(0)}k_2^2)$$

$$M_{7\ 10} = -(e_2^{(1)}k_2^4 + 4e_2^{(0)}k_2^3)$$

$$M_{87} = -(e_2^{(2)}k_2 + 2e_2^{(1)})$$

$$M_{88} = -(e_2^{(2)}k_2^2 + 4e_2^{(1)}k_2 + 2e_2^{(0)})$$

$$M_{89} = -(e_2^{(2)}k_2^3 + 6e_2^{(1)}k_2^2 + 6e_2^{(0)}k_2)$$

$$M_{8\ 10} = -(e_2^{(2)}k_2^4 + 8e_2^{(1)}k_2^3 + 12e_2^{(0)}k_2^2)$$

$$M_{97} = -(e_2^{(3)}k_2 + 3e_2^{(2)})$$

$$M_{98} = -(e_2^{(3)}k_2^2 + 6e_2^{(2)}k_2 + 6e_2^{(1)})$$

$$M_{99} = -(e_2^{(3)}k_2^3 + 9e_2^{(2)}k_2^2 + 18e_2^{(1)}k_2 + 6e_2^{(0)})$$

$$M_{9\ 10} = -(e_2^{(3)}k_2^4 + 12e_2^{(2)}k_2^3 + 36e_2^{(1)}k_2^2 + 24e_2^{(0)}k_2)$$

$$M_{10\ 7} = -(e_2^{(4)}k_2 + 4e_2^{(3)})$$

$$M_{10\ 8} = -(e_2^{(4)}k_2^2 + 8e_2^{(3)}k_2 + 12e_2^{(2)})$$

$$M_{10\ 9} = -(e_2^{(4)}k_2^3 + 12e_2^{(3)}k_2^2 + 36e_2^{(2)}k_2 + 24e_2^{(0)})$$

$$M_{10\ 10} = -(e_2^{(4)}k_2^4 + 16e_2^{(3)}k_2^3 + 72e_2^{(2)}k_2^2 + 96e_2^{(1)}k_2 + 24e_2^{(0)})$$

In the above equations, $e^{(t)}$, the t^{th} derivative is obtained using the recursive relationship,

$$e^{(t)} = A^{-1}(k)\left[B^{(t)} - \sum_{q=0}^{t}(1-\delta_{qo})C_{t,q}A^{(q)}(k)e^{(t-q)}(k)\right] \tag{28}$$

$A^{(q)}(k)$ is the q^{th} derivative with respect to k of *A(k)* and $B^{(t)}(k)$ is the t^{th} derivative with respect to k of *B(k)*. The Kronecker delta δ_{qo} is defined as

$$\delta_{qo} = \begin{cases} 1 & q = 0 \\ 0 & q \neq 0 \end{cases} \tag{29}$$

The frequency derivatives of *A(k)* and *B(k)* are evaluated and given in [6].

The above procedure can be generalized for multiple frequencies with frequency-derivatives evaluated at each frequency to increase the accuracy of the rational function. Alternatively, the two-frequency-four-derivative model can be used with multiple frequency windows. As the complexity of the matrix equation to solve for multiple-frequency-multiple derivative model increases with the number of frequency points and number of derivatives taken at each frequency, the two-frequency-four-derivative model is followed in this report.

3. Numerical Results

To validate the analysis presented in the previous sections, a few numerical examples are considered. Calculation of input characteristics over a frequency range are done for an open

coaxial line, coaxial cavity, and cavity-backed square and circular microstrip patch antennas. The numerical data obtained using MBPE are compared with the results calculated at each frequency using the computer code CBS3DR[12], which implements the combined FEM/MoM technique[2]. We will refer to the latter method as "exact solution." Due to the hybrid FEM/MoM technique, matrix $A(k_o)$ is partly sparse and partly dense. The Complex Vector Sparse Solver (CVSS) [13] is used to LU factor the matrix $A(k_o)$ once, and the moments are obtained by backsolving the equation (28) with multiple right-hand sides. All the computations reported below are done on a SGI *Indigo2* (with IP22 processor) computer.

(a) Open Coaxial line:

An open coaxial line radiating into an infinite ground plane (fig. 3a) is considered. A finite length of the line is used for FEM discretization. The input plane S_{inp} is placed at $z = 0$ plane and the radiating aperture at $z = 1cm$. The discretization of the coaxial line resulted in 1119 total unknowns, and the order of the dense matrix due to MoM is 144. One-frequency MBPE with *L=5* and *M=4* at f_o=7.5GHz is used to calculate the frequency response of the input admittance. Two-frequency MBPE at f_1=6GHz and f_2=9GHz with *L=5* and *M=4* is also used to calculate the frequency response. The frequency response over the frequency range 1GHz-13GHz is plotted in Figure 3(b) along with the exact solution calculated at 23 discrete frequency points over this frequency range. Both one-frequency and two-frequency MBPE frequency responses are calculated at 0.1GHz increments. One-frequency MBPE took 97 secs to generate moments, whereas two-frequency MBPE took a total of 166 secs to generate the moments at both frequencies. The exact solution took 990 secs to calculate input admittance at 23 frequency values from 1GHz to 13GHz. It can be seen that one-frequency MBPE agrees well with the exact solution over the frequency range 4.5GHz to 13GHz, whereas two-frequency MBPE agrees well

with the exact solution over the frequency range 1GHz to 13GHz. Both one-frequency MBPE and two-frequency MBPE are faster than the exact solution over the frequency range. Two-frequency MBPE has advantage over the one-frequency MBPE as it requires less computer memory[1].

(b) Open Coaxial Cavity:

An open coaxial cavity fed by a 50Ω coaxial line (fig. 4) is considered as a second example. The input plane S_{inp} is placed at $z = 0$ plane and the radiating aperture at $z = 0.952cm$ plane. The cavity volume is discretized using tetrahedral elements, which resulted in 4541 total unknowns and the order of the dense matrix due to MoM is 666. The frequency response of the return loss ($=20\log|\Gamma|$) is calculated using one-frequency MBPE with *L=5* and *M=4* at f_o=7.5GHz and is plotted in Figure 5. Two-frequency MBPE with *L=5* and *M=4* at f_1=6GHz and f_2=10GHz is also used to calculate the frequency response of the return loss along with the exact solution calculated at 24 frequency points over the frequency range 1GHz to 13GHz. It can be seen that the one-frequency MBPE agrees well with the exact solution over the frequency range 1GHz to 10GHz, whereas the two-frequency MBPE agrees well with the exact solution over the frequency range 1GHz to 13GHz. Both one-frequency and two-frequency MBPE frequency responses are calculated with 0.1GHz increments. One-frequency MBPE took 1563 secs to generate the moments, whereas two-frequency MBPE took a total of 2834 secs to generate the moments at both frequencies. The exact solution took a total of 18,576 secs to calculate return loss at 24 frequency points in the frequency range 1GHz to 13GHz. Both one-frequency MBPE and two-frequency MBPE are faster than the exact solution for the frequency response calculation.

1. Please see the comment on storage at the end of this section for detailed explanation.

(c) Cavity-Backed Square Microstrip Patch Antenna:

A cavity-backed square microstrip antenna radiating into an infinite ground plane (fig. 6) is considered. The input plane S_{inp} is placed at $z = 0$ plane and the radiating aperture at $z = 0.16cm$. The discretization of the cavity volume resulted in 2,160 total unknowns and the order of the dense matrix due to MoM is 544. The frequency response of the input impedance $(1/Y_{in})$ is calculated using one-frequency MBPE with L=5 and M=4 at f_o=4GHz and also using two-frequency MBPE with L=5 and M=4 at f_1=3GHz and f_2=5GHz. The numerical data are plotted in Figure 7 along with the exact solution calculated at 23 frequency points over the frequency range 1GHz to 7GHz. It can be seen from Figure 7 that one-frequency MBPE agrees well with the exact solution over the frequency range 1GHz to 6GHz, whereas the two-frequency MBPE agrees well with the exact solution over the frequency range 1GHz to 7GHz. Both one-frequency and two-frequency MBPE frequency responses are calculated with 0.01GHz increments. One-frequency MBPE took 1107 secs of CPU time to generate the moments, whereas the two-frequency MBPE took a total of 1120 secs of CPU time to generate moments at both frequencies. The exact solution took a total of 11,891 secs of CPU time for computations at 23 frequency points over the frequency range 1GHz to 7GHz. One-frequency MBPE and two-frequency MBPE are faster than the exact solution for the frequency response calculations.

(d) Cavity-Backed Circular Microstrip Patch Antenna:

A cavity-backed circular microstrip antenna radiating into an infinite ground plane is shown in Figure 8. The input plane S_{inp} is placed at $z = 0$ plane and the radiating aperture at $z = 0.16cm$. The discretization of the cavity volume resulted in 6,363 total unknowns and the order of the dense matrix due to MoM is 469. The frequency response of the input impedance $(1/Y_{in})$ is calculated using one-frequency MBPE with L=5 and M=4 at f_o=6GHz and also using

two-frequency MBPE with L=5 and M=4 at f_1=5GHz and f_2=7GHz. The numerical data are plotted in Figure 9 along with the exact solution calculated at 17 frequency points over the frequency range 3GHz to 9GHz. It can be seen from Figure 9 that one-frequency MBPE and two-frequency MBPE agree well with the exact solution over the frequency range 3GHz to 9GHz. Both one-frequency and two-frequency MBPE frequency responses are calculated with 0.01GHz increments. One-frequency MBPE took 913 secs of CPU time to generate the moments, whereas the two-frequency MBPE took a total of 1636 secs of CPU time to generate moments at both frequencies. The exact solution took a total of 7,650 secs of CPU time for computations at 18 frequency points over the frequency range 3GHz to 9GHz. One-frequency MBPE and two-frequency MBPE are faster than the exact solution for the frequency response calculations.

Comment on Storage: In all the above examples, when solving a matrix equation, one needs to store a complex, partly sparse and partly dense matrix $A(k_o)$ for exact solution at each frequency. In one-frequency MBPE one needs to store the derivative matrices ($A^{(q)}(k_o)$, *q=1,2,3,...(L+M)*), along with the matrix $A(k_o)$. For electrically large problems, this could impose a burden on computer resources. This problem can be overcome by storing the derivative matrices, $A^{(q)}(k_o)$ out-of-core, as the derivative matrices are required only for matrix-vector multiplication. In two-frequency MBPE, one needs to store only $\left(\frac{L+M-1}{2}\right)$ derivative matrices along with the matrix $A(k)$ at each frequency. Once the moments are calculated at one frequency, the memory used for the matrices can be reutilized to generate moments at the second frequency, hence reducing the burden on computer memory requirements. In all the numerical examples presented with *L=5* and *M=4*, one-frequency MBPE had to store 10 matrices, whereas two frequency-MBPE had to store only 5 matrices at each frequency. The memory to store the

matrices at one frequency is reutilized to store the matrices at the second frequency. Hence, even though the CPU timings for two-frequency MBPE is more than the one-frequency MBPE, if computer memory is a constraint, it is advisable to use two-frequency MBPE as an alternative to one-frequency MBPE.

4. Concluding Remarks

The MBPE technique is applied to the hybrid FEM/MoM technique to obtain the frequency response of the input characteristics of cavity-backed aperture antennas. The frequency response of input characteristics of an open coaxial line, coaxial cavity, square microstrip patch antenna, and a circular patch antenna are computed and compared with the exact solution. From the numerical examples presented in this work, MBPE technique is found to be superior in terms of CPU time to obtain a frequency response. It may be noted that although calculations are done in frequency increments of 0.1GHz or 0.01GHz for the examples presented, the frequency response at even finer frequency increments can also be calculated with a very nominal cost. In one-frequency MBPE, the frequency response is valid over a certain frequency range. In two-frequency MBPE, the two frequency values have to be chosen so as to get an accurate frequency response between the two frequency values. To get a wide frequency response for any problem, either one- or two-frequency MBPE models have to be used with different frequency values to cover the complete frequency range. To be accurate over all frequency ranges, a reliable error criteria should be developed, which can be used to sample the frequency points to apply MBPE model. Development of such a sampling criteria will make MBPE a very effective tool for computational electromagnetics.

References

[1] J. M. Jin and J. L. Volakis, "A hybrid finite element method for scattering and radiation by microstrip patch antennas and arrays residing in a cavity," *IEEE Trans. Antennas and Propagation*, Vol.39, pp.1598-1604, November 1991.

[2] C. J. Reddy, M. D. Deshpande, C. R. Cockrell and F. B. Beck, "Radiation characteristics of cavity backed aperture antennas in finite ground plane using the hybrid FEM/MoM technique and geometrical theory of diffraction," *IEEE Trans. Antennas and Propagation*, Vol.44, pp.1327-1333, October 1996.

[3] E. Chiprout and M. S. Nakhla, *Asymptotic Waveform Evaluation*, Kulwar Academic Publishers, 1994.

[4] C.R.Cockrell and F.B.Beck, "Asymptotic Waveform Evaluation (AWE) technique for frequency domain electromagnetic analysis," *NASA Technical Memorandum 110292*, November 1996.

[5] C. J. Reddy and M. D. Deshpande, "Application of AWE for RCS frequency response calculations using Method of Moments," *NASA Contractor Report 4758*, October 1996.

[6] C.J.Reddy and M.D.Deshpande, "Frequency response calculations of input characteristics of cavity-backed aperture antennas using AWE with hybrid FEM/MoM technique," *NASA Contractor Report 4764*, February 1997.

[7] G.J.Burke, E.K.Miller, S.Chakrabarthi and K.Demarest, "Using model-based parameter estimation to increase the efficiency of computing electromagnetic transfer functions," *IEEE Trans. Magnetics*, Vol.25, pp.2807-2809, July 1989.

[8] E.K.Miller and G.J.Burke, "Using model-based parameter estimation to increase the physical interpretability and numerical efficiency of computational electromagnetics,"

Computer Physics Communications, Vol.68, pp.43-75, 1991.

[9] R.F.Harrington, *Time Harmonic Electromagnetic Fields*, McGraw Hill Inc, 1961.

[10] C.J.Reddy, M.D.Deshpande, C.R.Cockrell and F.B.Beck, "Finite element method for eigenvalue problems in electromagnetics," *NASA Technical Paper 3485*, December 1994.

[11] C.J.Reddy and M.D.Deshpande, "Application of AWE along with a combined FEM/MoM technique to compute RCS of cavity-backed aperture in an infinite ground plane over a frequency range," *NASA Contractor Report 97-206261*, December 1997.

[12] C.J.Reddy and M.D.Deshpande, "User's Manual for CBS3DR-Version 1.0," *NASA Contractor Report 198284*, February 1996.

[13] O. O. Storaasli, "Performance of NASA equation solvers on computational mechanics applications," *American Institute of Aeronautics and Astronautics (AIAA) Paper No. 96-1505*, April, 1996

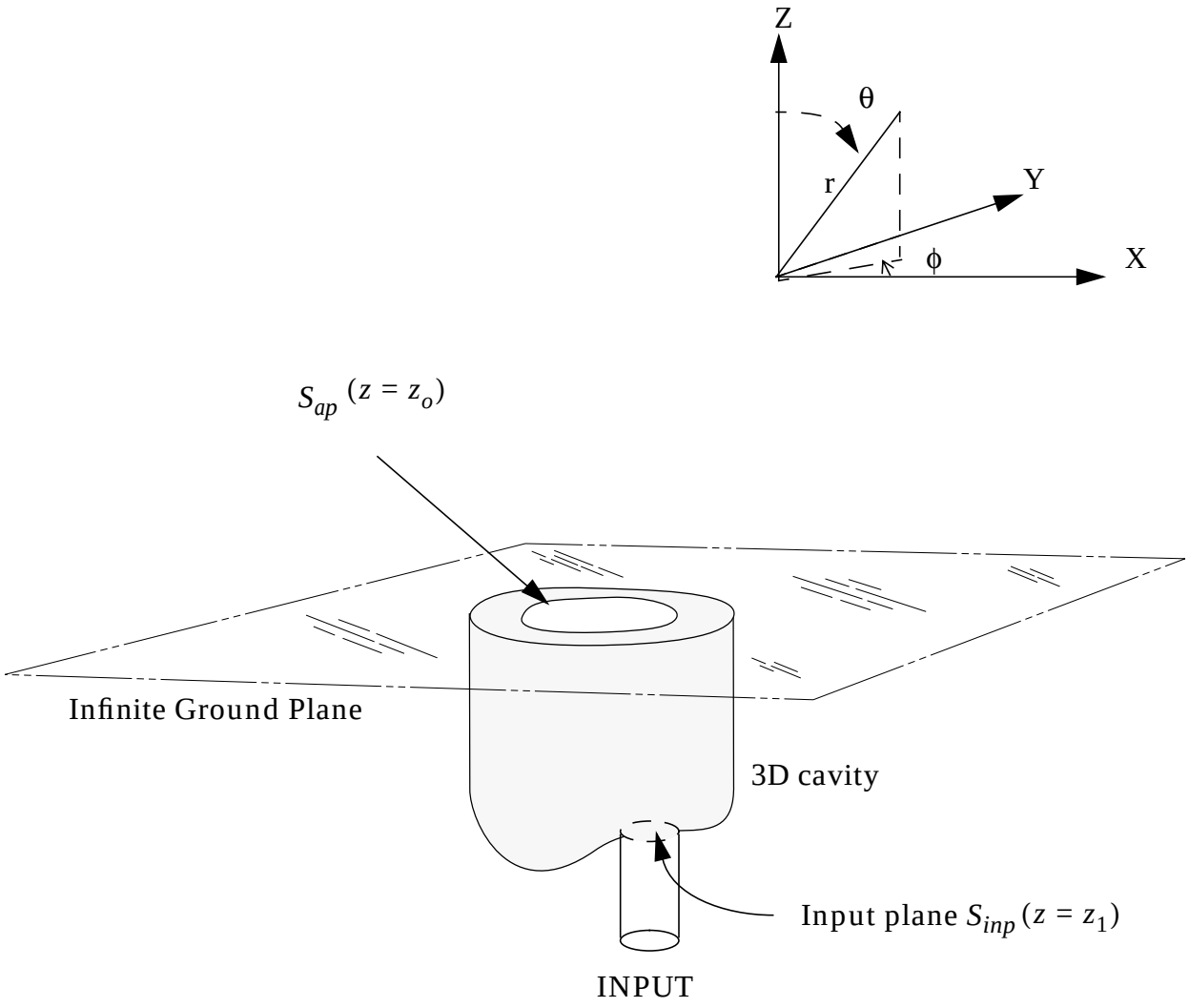

Figure 1 Geometry of a cavity backed aperture in finite ground plane.

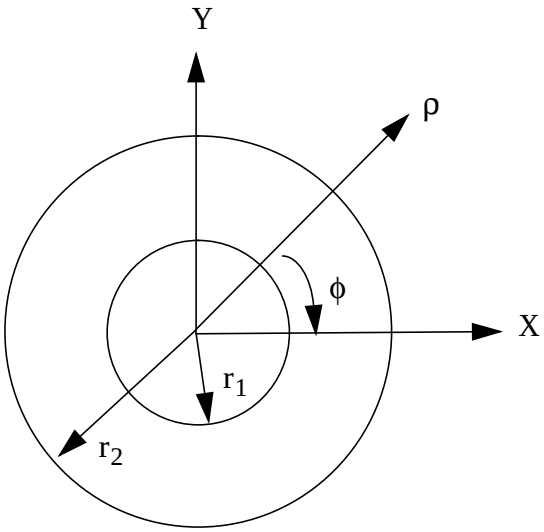

Figure 2 Cross section of the coaxial line.

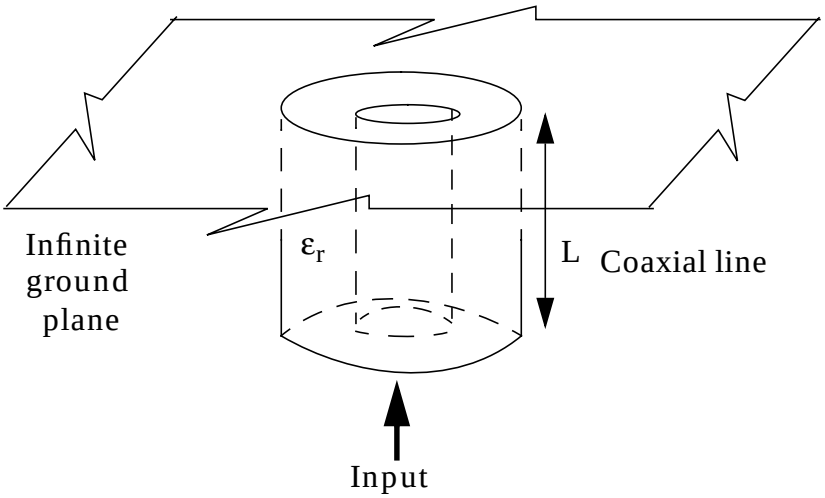

(a)

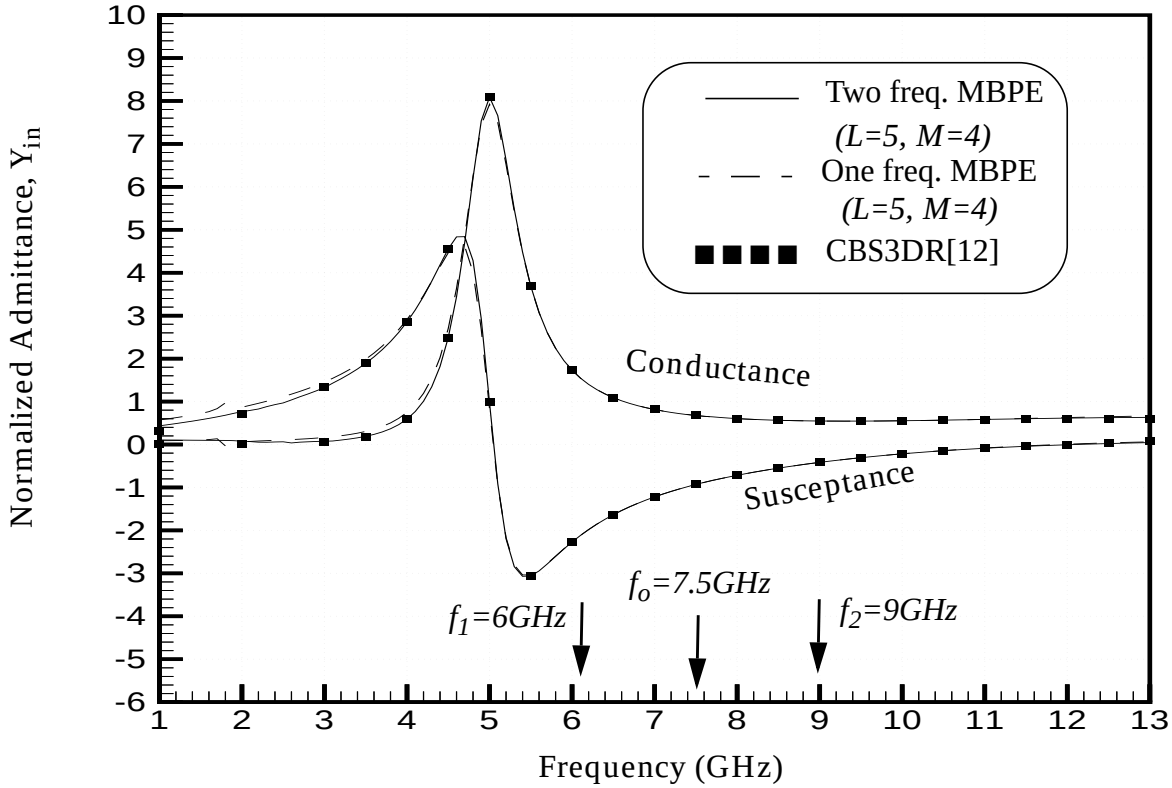

(b)

Figure 3 (a) Open coaxial line in an infinite ground plane. Inner radius r_1=1cm, Outer radius r_2=1.57cm, ε_r =1.0 and L=1.0cm

(b) Normalized input admittance as a function of frequency.

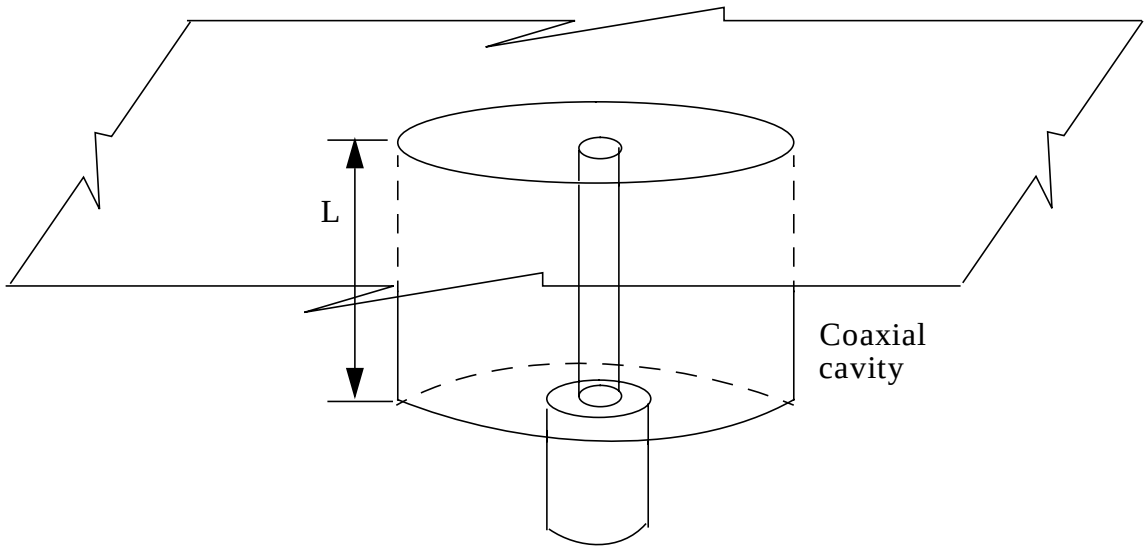

Figure 4 Geometry of a coaxial cavity in an infinite ground plane. Outer radius of the coaxial cavity=1", Inner radius of the coaxial cavity=0.0181" and L=3/8". The cavity is fed by a 50Ω coaxial line.

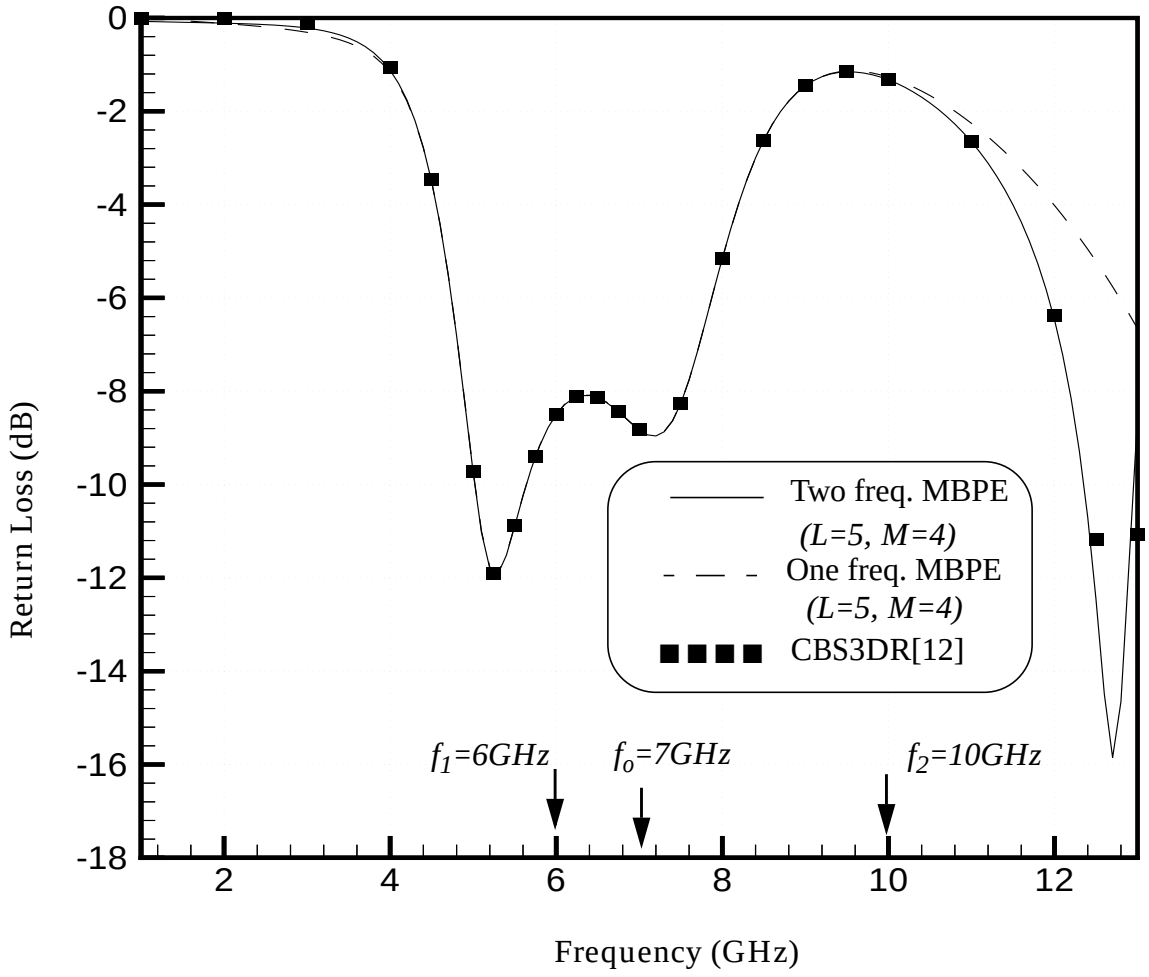

Figure 5 Return loss versus frequency of the coaxial cavity (figure 4).

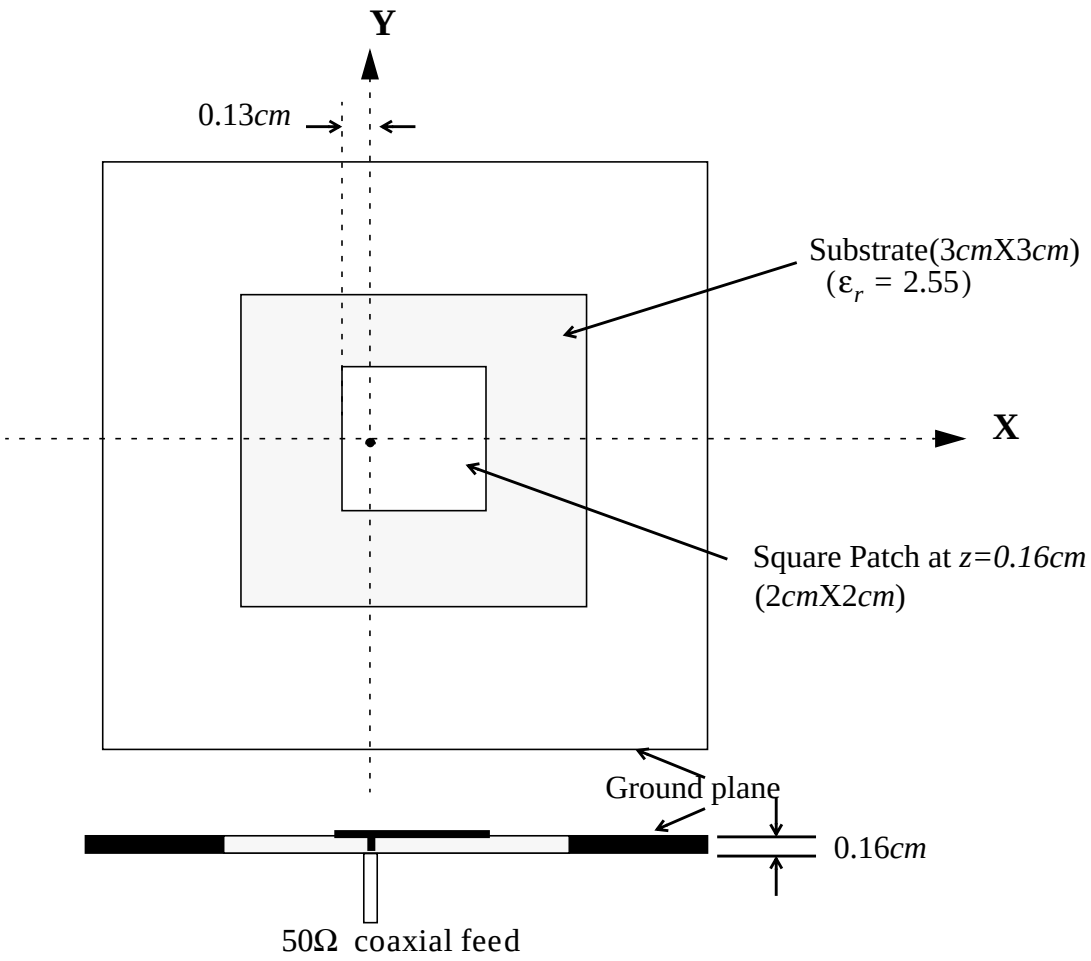

Figure 6 Cavity-backed square microstrip patch antenna in an infinite ground plane fed by a 50Ω coaxial line.

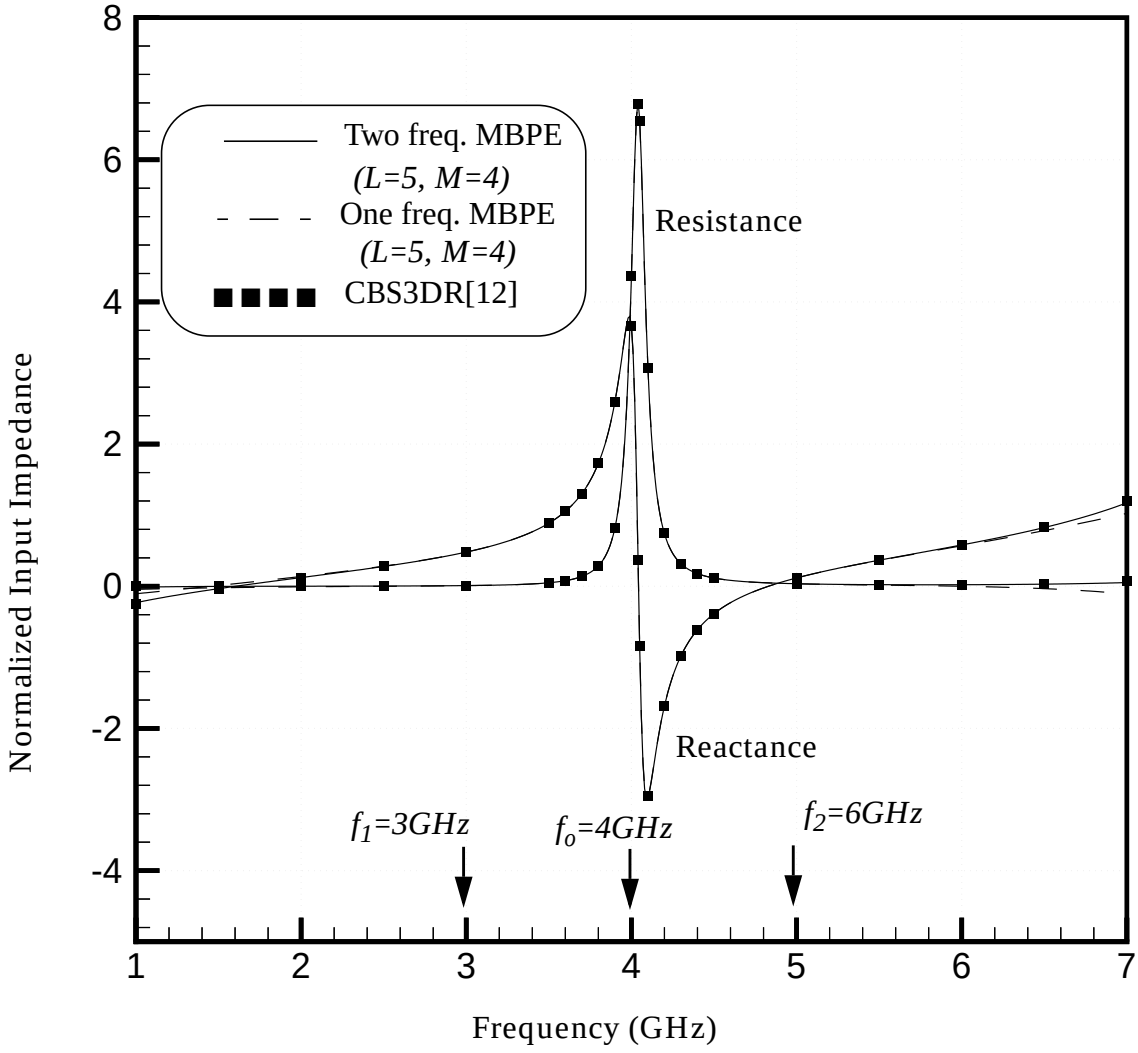

Figure 7 Normalized input impedance versus frequency of the cavity-backed square microstrip antenna (figure 6).

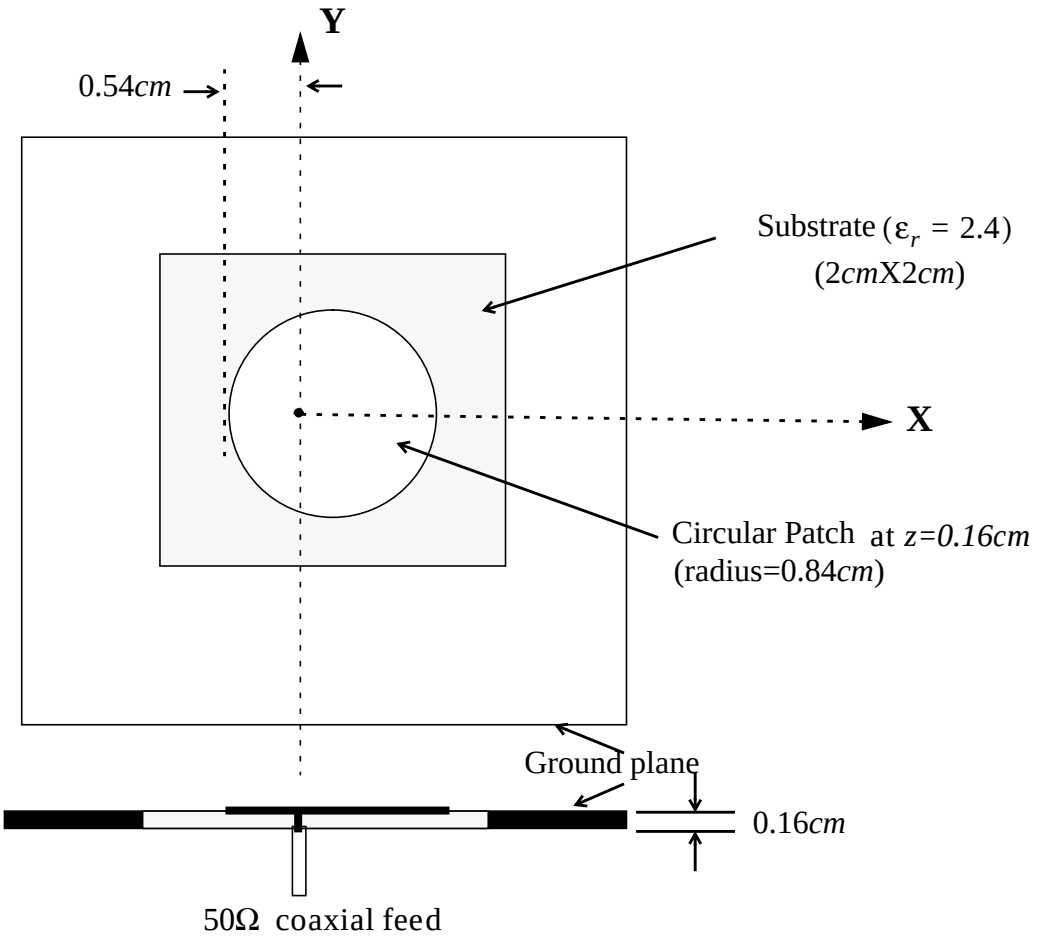

Figure 8 Cavity-backed circular microstrip patch antenna in an infinite ground plane fed by a 50Ω coaxial line.

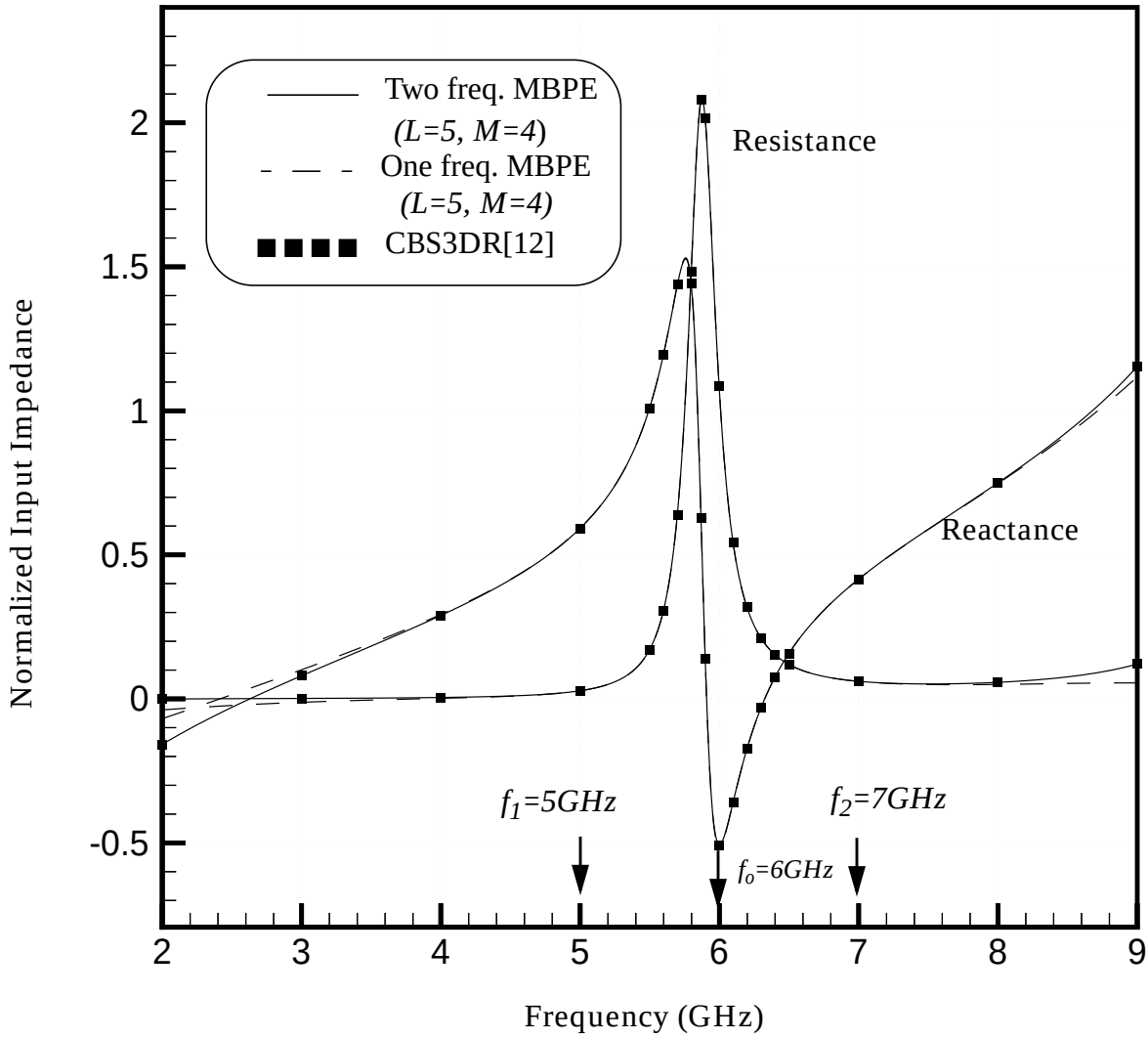

Figure 9 Normalized input impedance versus frequency of the cavity-backed circular microstrip antenna (figure 8).

REPORT DOCUMENTATION PAGE

Form Approved
OMB No. 07704-0188

1. AGENCY USE ONLY *(Leave blank)*	2. REPORT DATE	3. REPORT TYPE AND DATES COVERED
	March 1998	Contractor Report

4. TITLE AND SUBTITLE
Application of Model Based Parameter Estimation for Fast Frequency Response Calculations of Input Characteristics of Cavity-Backed Aperture Antennas Using Hybrid FEM/MoM Technique

5. FUNDING NUMBERS
NCC1-231

522-11-41-02

6. AUTHOR(S)
C. J. Reddy

7. PERFORMING ORGANIZATION NAME(S) AND ADDRESS(ES)
Hampton University
Hampton, Virginia 23668

8. PERFORMING ORGANIZATION REPORT NUMBER

9. SPONSORING/MONITORING AGENCY NAME(S) AND ADDRESS(ES)
National Aeronautics and Space Administration
Langley Research Center
Hampton, VA 23681-2199

10. SPONSORING/MONITORING AGENCY REPORT NUMBER
NASA/CR-1998-206950

11. SUPPLEMENTARY NOTES
Langley Technical Monitor: Fred B. Beck

12a. DISTRIBUTION/AVAILABILITY STATEMENT
Unclassified–Unlimited
Subject Category 32 Distribution: Nonstandard
Availability: NASA CASI (301) 621-0390

12b. DISTRIBUTION CODE

13. ABSTRACT ***(Maximum 200 words)***

Model Based Parameter Estimation (MBPE) is presented in conjunction with the hybrid Finite Element Method (FEM)/Method of Moments (MoM) technique for fast computation of the input characteristics of cavity-backed aperture antennas over a frequency range. The hybrid FEM/MoM technique is used to form an integro-partial-differential equation to compute the electric field distribution of a cavity-backed aperture antenna. In MBPE, the electric field is expanded in a rational function of two polynomials. The coefficients of the rational function are obtained using the frequency derivatives of the integro-partial-differential equation formed by the hybrid FEM/MoM technique. Using the rational function approximation, the electric field is obtained over a frequency range. Using the electric field at different frequencies, the input characteristics of the antenna are obtained over a wide frequency range. Numerical results for an open coaxial line, probe-fed coaxial cavity and cavity-backed microstrip patch antennas are presented. Good agreement between MBPE and the solutions over individual frequencies is observed.

14. SUBJECT TERMS
Model Based Parameter Estimation (MBPE), Padé Approximation, FEM, MoM, Hybrid Method, Cavity-Backed Aperture Antennas, Input Admittance

15. NUMBER OF PAGES
38

16. PRICE CODE
A03

17. SECURITY CLASSIFICATION OF REPORT	18. SECURITY CLASSIFICATION OF THIS PAGE	19. SECURITY CLASSIFICATION OF ABSTRACT	20. LIMITATION OF ABSTRACT
Unclassified	Unclassified	Unclassified	